

Size-dependent anisotropic diamagnetic screening in superconducting Sn nanowires

T. G. Sorop* and L. J. de Jongh†

Kamerlingh Onnes Laboratory, Leiden University, 2300 RA Leiden, The Netherlands

(Received 28 June 2006; revised manuscript received 9 September 2006; published 9 January 2007)

We present orientation dependent magnetic measurements on ordered arrays of parallel Sn nanowires for diameters $D \approx 6$ –170 nm. For $D \geq 50$ nm clear superconducting transitions could be detected below $T_c = 3.7$ K attributed to superconductivity of the individual nanowires. Decreasing the wire diameters from bulk values to 50 nm strongly reduces the diamagnetism (by a factor of 10^4) and enhances the critical field by a factor of 45. For magnetic fields parallel and perpendicular to the wire axis we detect an anisotropy in the diamagnetic screening that is enhanced with decreasing D far above the Ginzburg-Landau prediction. This behavior is attributed to size-dependent anisotropy in the electronic mean free path.

DOI: [10.1103/PhysRevB.75.014510](https://doi.org/10.1103/PhysRevB.75.014510)

PACS number(s): 74.81.Fa, 74.25.Ha, 74.78.Na

I. INTRODUCTION

A subject of vivid current interest is how the physical properties of nanowires or nanoparticles are affected by a progressive reduction of the system size. For superconductors this occurs when the sample dimensions become comparable with the coherence length ξ , or the penetration depth λ .¹ A problem of actual theoretical² research is whether superconductivity can survive in very narrow nanowires and, if not, at what critical diameter will it disappear. Recently, thanks to advances in nanotechnology, it has become possible to study this issue also experimentally. Various methods, such as nanolithography,³ nanotube templating,⁴ physical vapor deposition,⁸ and DNA templating⁵ have been exploited to fabricate single superconducting nanowires. In recent studies nanoporous track-etched polymers^{6,7} and nanoporous alumina⁹ have been used as templates for two-dimensional (2D) arrays of wires. Apart from transport measurements such arrays offer attractive possibilities of performing magnetic measurements using bulk techniques.

In this work, we study the size-dependent superconductivity of 2D arrays of Sn nanowires embedded in nanoporous alumina templates. These templates have the advantage that all pores are strictly parallel and well-isolated from one another in a hexagonal regular array. In addition, the method allows good control over the diameter, and ensures very narrow size distribution and high aspect ratios. Our pore diameters extended from 6 to 170 nm, with lengths of the order of 1–10 μm . The pores were filled with Sn using the ac electroplating procedure described in detail in Refs. 10 and 11. Electron microscopy (scanning and transmission) confirmed that the pores are uniform in size, are well-separated, and form a regular hexagonal array. Mössbauer spectroscopy showed the Sn inside the pores to have the metallic β -Sn-phase. Only a few percent of the Sn was found to be oxidized, likely corresponding to surface layers at the cylinder walls. The filling fraction of the nanopores was determined by neutron activation analysis measurements, which revealed that only a small fraction of the pores, 3%–15%, is filled with Sn, the others being empty. On the other hand, for the filled pores the filling was found to be indeed from top to bottom. An attractive property of these membranes is, therefore, that they allow one to perform orientationally depen-

dent studies on a macroscopically large assembly of nearly identical nanowires. Thus one can exploit experimental methods normally used for bulk and yet measure properties that, as we will show, correspond, to a high degree of approximation, to individual nanowires. By performing magnetization measurements parallel and perpendicular to the wire axis, we detect a surprisingly large anisotropy in the diamagnetic screening properties, that, moreover, increases drastically with decreasing size. An explanation in terms of a size-dependent anisotropy in the mean free path is proposed.

II. EXPERIMENTAL DETAILS

Magnetic measurements were performed using a commercial superconducting quantum interference device (SQUID) magnetometer. All data were corrected for background contributions from sample holder and membrane, which had to be done carefully since, due to the small filling fraction and low shielding, the Sn signal was of the same order as, or even smaller than, the background. In fact, for wires with $D < 50$ nm, the diamagnetic screening was found too small to either prove or disprove the occurrence of superconductivity.

We first argue that the properties measured correspond to those of individual (noninteracting) nanowires. Since the interwire distance in our Al_2O_3 matrix is $d_i = 1.7D$, and thus a few tens of nanometers, and since no overlayer of Sn on top of the membranes was present, no conducting pathways between Sn wires exist. Therefore, in zero field, they act as individual isolated superconducting needles. Nevertheless, the diamagnetic moments created in each of the nanowires by the external magnetic field will exert dipolar magnetic fields at the neighboring sites. It turns out, however, that for both parallel and perpendicular orientations of the field these interactions can be neglected. For a parallel field, one may borrow from an argument known for ferromagnetic nanowires (see Refs. 11 and 12). The interwire dipolar field, which acts as a demagnetizing field, is approximately given by $\mathbf{H}_d = \gamma P \mathbf{M}_\parallel$, where P is the porosity of the structure, defined as $P = (\pi\sqrt{3}D^2/6d_i^2)$, and \mathbf{M}_\parallel the (volume) magnetization. The value of γ , which is in between 0 and 1, depends on the filling fraction. With $d_i = 1.7D$, it follows that γP can have a maximum value of 0.3. In our templates the filling

fractions are of order 10%; thus the product γP does not exceed 0.10, so that $H_d \ll H$.

We mention here that, although the filling fraction for our templates is rather low (3%–15%), the sample shows regions with almost all the pores completely filled with nanowires, separated by regions where all the pores are empty. Because the superconducting nanowires are embedded in such almost completely filled regions (containing tens to hundreds of wires) we argue that, in contrast to the case of completely random filling of the matrix, in our case the estimation of H_d is *relevant*.

For a perpendicular field, knowing the current distribution inside the cylinder, one can estimate with the Biot-Savart formula¹³ the dipolar field produced outside. Given the high aspect ratio, we adopt the approximation of an infinitely long cylinder, obtaining in cylindrical coordinates $\mathbf{H}_d(\rho, \varphi, z) = -\frac{M_\perp R^2}{4\pi \rho^2}(\cos 2\varphi \hat{x} + \sin 2\varphi \hat{y})$, where ρ is the radial distance and φ the angle between the field and \vec{r} . From this expression it can be easily seen that the contributions from the six nearest neighbors *exactly* cancel due to the hexagonal symmetry. The same is true, of course, for the second nearest neighbors and so forth. This at first sight perhaps unexpected result is in fact also valid for a quadratic lattice. Although experimentally the cancellation will not be complete, for instance, because of the inhomogeneous filling of the pores, one may conclude that the magnetic responses obtained should, to a good approximation, correspond to (averages over) individual, i.e., noninteracting, wires.

III. RESULTS AND DISCUSSIONS

As representative results we show in Figs. 1(a) and 1(b) data for $D=50$ and 170 nm, displaying the temperature dependence of the (dimensionless) dc volumetric susceptibility (defined as the ratio M/H ; for complete screening this would be -1). The data were obtained by cooling in zero field (ZFC) from 20 to 2 K and subsequently applying constant dc fields ($5 \text{ mT} < \mu_0 H < 5 \text{ T}$) parallel to the wire axis. The large diamagnetic signal found below 3.7 K can be unambiguously attributed to the superconducting transition of the Sn nanowires inside the matrix. As expected, the Meissner signal is reduced with increasing field and disappears completely above a critical field H_c , at which the sample enters the normal state. Since for parallel field the demagnetizing factor of our high aspect-ratio nanowires is basically zero, the observed diamagnetic signals directly give the Meissner shielding fractions. This fraction is already quite small (10^{-2}) for $D=170$ nm and decreases by two orders of magnitude when D is further reduced to 50 nm. The diamagnetic signal is then as small as 10^{-10} Am^2 (in units of magnetic moment), and for $D < 50$ nm it proved no longer possible to detect it in our SQUID magnetometer. We note that the critical temperature found is the same as in bulk Sn, $T_c=3.7$ K, independent of D . This agrees with previous studies of superconductors in confined geometries.⁷⁻⁹ By contrast, the field needed to completely suppress the superconducting state greatly exceeds the bulk Sn value (at $T=2$ K) of $\mu_0 H_{cb}=28$ mT (see below).

Quite similar conclusions can be drawn from the magnetization curves measured in parallel field at constant tem-

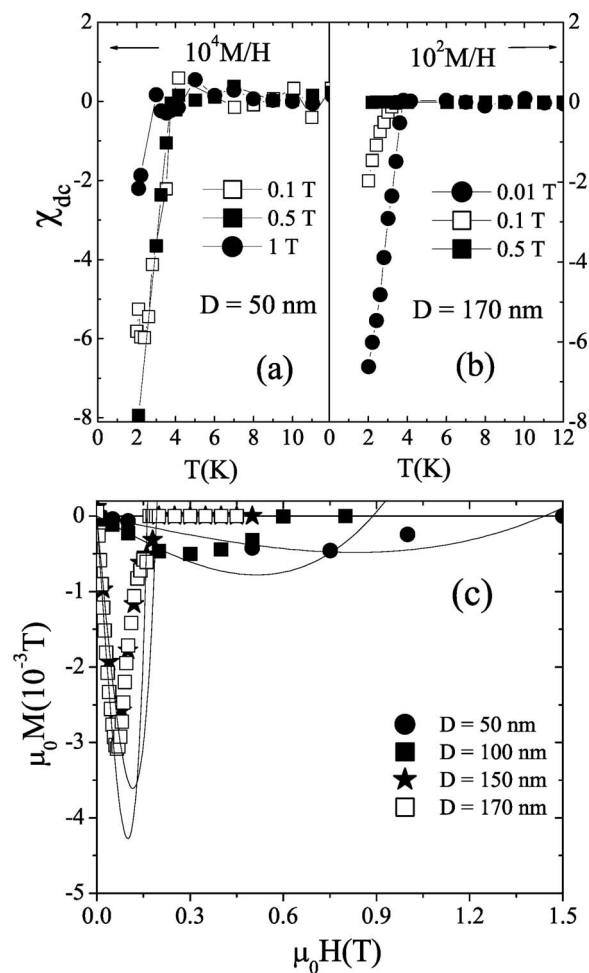


FIG. 1. (a) and (b) dc volumetric susceptibility (in Systeme International units) in parallel constant fields as a function of temperature for wires with (a) $D=50$ nm and (b) $D=170$ nm. (c) Magnetization ($T=2$ K) as a function of field for different diameters. The experimental data (symbols) are compared with the Ginzburg-Landau fits (straight lines), with λ as adjustable parameter.

perature, shown in Fig. 1(c) for $T=2$ K. These data were measured applying the field-up (FU) procedure: first ZFC from 20 K down to 2 K and then sweeping the field up at constant temperature. We find a decrease of the initial susceptibility χ_i (defined as the initial slope of the magnetization curve) by more than two orders of magnitude when D is varied from 170 to 50 nm, in good agreement with the M vs T data. Furthermore, a strong enhancement of H_c upon reducing D is observed. Other authors⁶ have reported similar sharp reductions of the Meissner effect when the dimensions of the samples become comparable to or even lower than the penetration depth. This can be qualitatively understood by considering that the superconducting screening currents responsible for diamagnetism become limited by the finite sample size. Consequently, the diamagnetic screening becomes incomplete and the field needed to bring the superconductor in the normal state will increase. A compilation of the data found for the dependence on D of the χ_{init} for parallel field is given in Fig. 2(a). Further, the strong enhancement of the parallel critical field with decreasing D is illustrated in

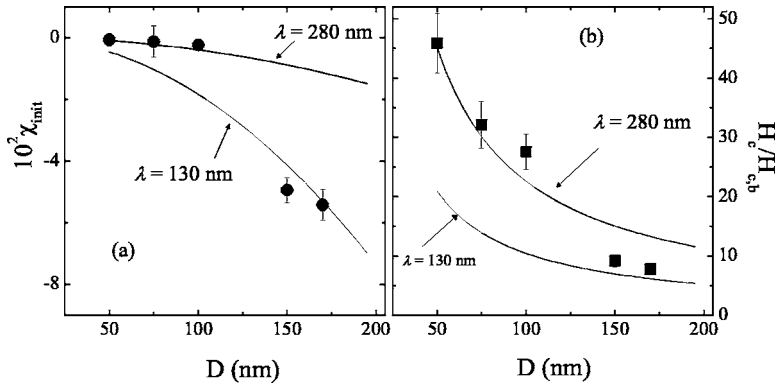


FIG. 2. (a) Initial susceptibility and (b) critical field data as a function of D as determined from Fig. 1(c). Curves are Ginzburg-Landau fits for different choices of λ . All data were taken in parallel field at $T=2$ K.

Fig. 2(b). The experiment shows that $\mu_0 H_c \approx 1$ T for $D = 50$ nm (at $T=2$ K), which, when compared to the bulk value of 28 mT, presents an enhancement factor of more than 45.

We next turn to another prominent outcome of the experiment, which is the unexpectedly large anisotropy observed in the diamagnetic screening properties. To our knowledge such orientationally dependent magnetic studies have not been previously performed in superconducting nanowires with

such small diameters. The anisotropy in the diamagnetic screening becomes particularly apparent in the M vs H data shown in Figs. 3(a) and 3(b), in which representative results for two diameters ($D=50$ and 170 nm) are plotted for both parallel and perpendicular fields. It is obvious, in particular from Fig. 3(b), that the critical field (as determined from the point at which the M vs H curve joins the field axis $M=0$) is largest in the parallel case for which also χ_i is smaller. When varying D , we find again these differences to become more

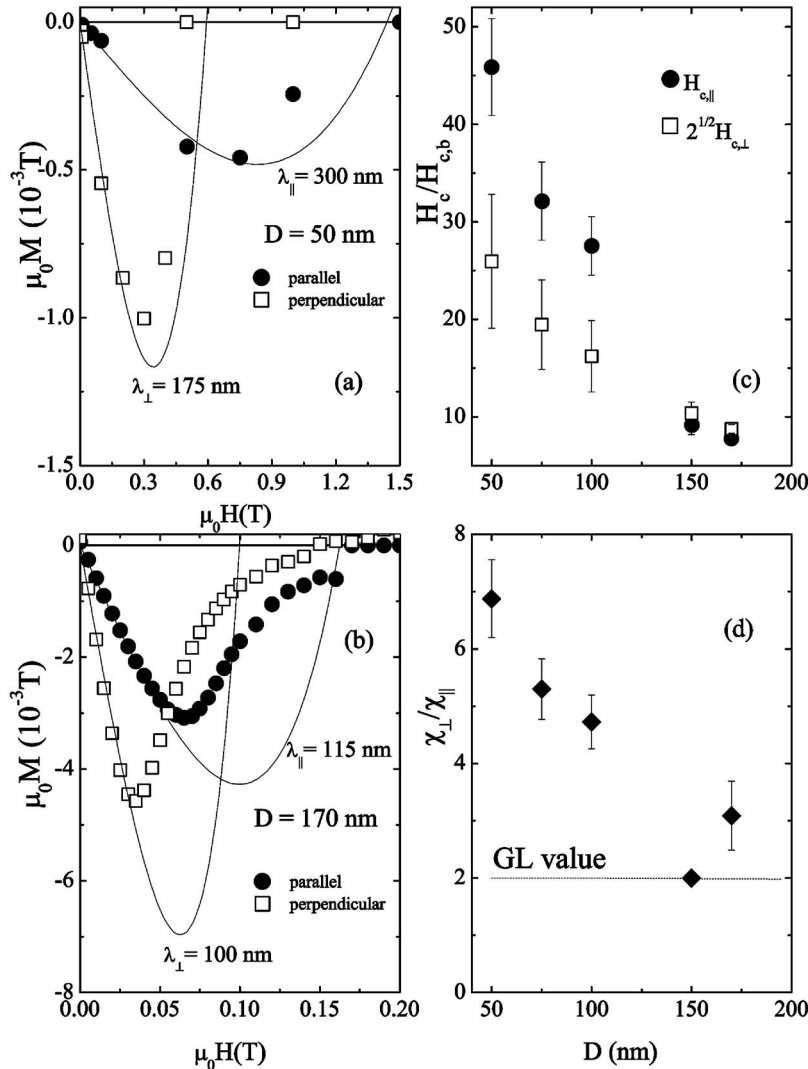


FIG. 3. Comparison between parallel and perpendicular diamagnetic screening ($T=2$ K). (a) and (b) Magnetization curves for (a) $D=50$ nm and (b) $D=170$ nm. The experimental data (symbols) are compared with the Ginzburg-Landau fits (solid curves). (c) Diameter dependence of the critical field for parallel and perpendicular field orientations. $H_{c,\perp}$ was multiplied by $\sqrt{2}$ to compare to GL prediction. (d) Idem for the ratio of perpendicular and parallel susceptibility. The dotted line indicates the GL prediction.

pronounced the smaller the diameter. To illustrate the anisotropy effect more quantitatively we have collected in Fig. 3(c) the H_c values obtained for all samples and for both orientations. Even though the error bars are large for smallest diameters, in particular for $H_{c,\perp}$, it can be concluded that the ratio $H_{c,\parallel}/H_{c,\perp}$ increases strongly with decreasing D . Further, in Fig. 3(d) we plot the ratio of initial susceptibilities $\chi_{\parallel}/\chi_{\perp}$ (estimated from M vs H curves) as a function of D , at $T=2$ K.

For theoretical analysis of data on samples of reduced dimensionality one usually takes the Ginzburg-Landau (GL) theory for the “dirty limit” as a starting point. This theory predicts the coherence length ξ and the penetration depth λ to depend on the electronic mean free path l_e as $\xi \propto (\xi_0 l_e)^{1/2}$ and $\lambda \propto \lambda_L(1 + \xi_0/l_e)^{1/2}$. For bulk Sn, a type I, BCS superconductor, the intrinsic coherence length $\xi_0=230$ nm and the London penetration depth $\lambda_L=34$ nm. For sufficiently pure superconductors in confined geometries, l_e becomes limited by the sample dimensions, here the wire diameter D . Consequently, ξ will decrease and λ will increase, the GL parameter $\kappa=\lambda/\xi$ will become larger than $1/\sqrt{2}$, and the material should turn into a type-II superconductor. For samples with defects (caused either by impurities or by noncrystallinity) l_e can be even smaller than D , leading to an even larger enhancement of κ . For small enough D the superconducting order parameter will be more or less constant over the sample width and the GL theory predicts^{14,15} a second order phase transition in field, as long as the diameter does not exceed a critical value, which is $D_c=\lambda\sqrt{3}$ for a cylinder. Our samples are all in the limit $D < D_c$. However, since for the temperatures probed in our experiments ($T \geq 2$ K) D is smaller than 2ξ (the size of a vortex core) we exclude the possibility of fitting (Abrikosov) vortices in our samples. Therefore for a quantitative analysis with GL theory, we first compare our data with the predictions of Silin¹⁷ for the specific case of a (small) cylindrical superconductor when considering only the (incomplete) Meissner effect. For $D \ll \lambda$, Silin found the magnetization to be given by¹⁶

$$\frac{M}{H} = -\frac{1}{a} \left(\frac{D}{\lambda}\right)^2 + \frac{1}{24a} \left(\frac{D}{\lambda}\right)^4 + \frac{1}{48a^2} \left(\frac{H}{H_{cb}}\right)^2 \left(\frac{D}{\lambda}\right)^6, \quad (1)$$

where a is a constant that depends on the orientation of the field:¹⁷ $a_{\parallel}=8$ and $a_{\perp}=4$ (H_{cb} is the bulk critical field).

The dependence of χ_i at $T=2$ K on D as plotted in Fig. 2(a) for parallel field has been fitted with the above equation, with λ as a free parameter. The results of two fitting curves are shown indicating a strong increase from $\lambda=130$ nm at high D to $\lambda=280$ nm at small D . The strong enhancement of the parallel critical field with decreasing D shown in Fig. 2(b) has likewise been fitted to Silin’s theory,² using his formula¹⁵ $H_c=b_D^{\lambda} H_{cb}$, with $b_{\parallel}=8$ and $b_{\perp}=8/\sqrt{2}$. Although the amount of experimental data is relatively small, we again find for $D < 100$ nm a value of $\lambda=280$ nm, whereas for $D > 150$ nm $\lambda=130$ nm gives a better fit, in agreement with the χ_{init} data. Using the dirty limit formula for λ we obtain mean free path values that are significantly smaller than the wire diameter. For the high diameters $l_e \approx 20$ nm, whereas for $D < 100$ nm $l_e \approx 4$ nm. A possible reason for such small l_e can

be the polycrystalline structure of the wires, where the crystalline regions would be smaller in size than the wire diameter. Indeed in the SEM studies the wires turn out to be polycrystalline. The variation of l_e with D may then be explained by a larger amount of structural defects for the smaller diameters.

We mention that recent papers^{8,9} have reported parallel critical fields in superconducting Sn nanowires as low as 0.3 T, for $D \approx 50$ nm. These wires were reported to be single-crystalline, which would imply that the l_e values were indeed limited by the wire diameters. In that case the l_e could be 10 times higher than ours, which explains why the critical fields, given by $H_c \propto l_e^{-1/2}$, are roughly three times smaller than those measured here.

When trying to fit the full measured magnetization curves to theory (with λ as an adjustable parameter) we find that our M vs H data in Figs. 1(c), 3(a), and 3(b) agree with Silin’s formula only at low H values, even if we include the higher-order terms in the formula.¹ The reason for this is not yet fully understood, but it might have to do with the fact that the Silin formulas are actually rigorously valid only in the limit $D \ll \lambda$. In our case this limit is much better obeyed for the smallest diameters, for which indeed the experimental data are closer to the fitting curves up to higher fields.

A striking result of the fits shown in Figs. 3(a) and 3(b) is the strong anisotropy in the values for the penetration depth obtained when fitting data for parallel and perpendicular fields for the same D . It should be stressed that in Silin’s theory an isotropic penetration depth is assumed. Within that assumption an anisotropy $H_{c,\parallel}/H_{c,\perp}=\sqrt{2}$ and $\chi_{\perp}/\chi_{\parallel}=2$ is predicted, independent of D , on the basis of cylindrical geometry. Contrastingly, the experimental ratio’s approach these limiting values only for large D , showing a strong increase for decreasing D . Since we are dealing with dirty superconductors, for which l_e is the relevant parameter, and since we have shown that $l_e < D$, we attribute these observations to an anisotropy in the mean free path. If, instead of a single isotropic l_e , we would assume different values, l_e^{\parallel} and l_e^{\perp} , corresponding to screening currents running parallel or perpendicular to the wire axis, the magnitude of the anisotropy would just be given by the ratio $l_e^{\parallel}/l_e^{\perp}$. This ratio is proportional to $\chi_{\perp}/\chi_{\parallel}$ and according to Fig. 3(c), increases when reducing the D , yielding values for $l_e^{\parallel}/l_e^{\perp}$ varying between 1 (at $D=150$ nm) and 3.4 (at $D=50$ nm). Similarly, the observed anisotropy in the critical fields can be expressed in terms of $l_e^{\perp}/l_e^{\parallel} \propto (H_{c,\parallel}/H_{c,\perp})^2$, yielding values of $l_e^{\perp}/l_e^{\parallel}$ between 0.8 (at highest D) and 3.2 (at lowest D). On the basis of the good agreement between these two results we conclude that $l_e^{\parallel} > l_e^{\perp}$ and that their ratio becomes larger when decreasing D . An explanation for this effect can be found on the basis of the polycrystalline structure of the wires and the particularity of the growth process. In view of the very high aspect ratio of the nanopores with smallest D , the growth process in the pores could be nonisotropic, leading to the columnar shape of the crystallites. In that case it is obvious that the electronic mean free path for screening currents running perpendicular to the wire axis (l_e^{\perp}) will be smaller than for currents running parallel (l_e^{\parallel}). Moreover, for larger D the growth mechanism should become more uniform, so that the

values of l_e would increase and become isotropic. Finally, they would become limited by D , in which limit the predictions of Silin for $l_e \geq D$ should be approached, as seen indeed in the experiment (cf. Fig. 3).

In conclusion, we mention that instead of the anisotropic Ginzburg-Landau theory used above, one may also turn to Usadel theory for diffusive mesoscopic superconductors.¹⁸ It can be shown¹⁹ that for cylindrical geometry the Usadel theory predicts $H_{c,\parallel} = \frac{2\sqrt{2}\Phi_0}{\pi D \xi_{\perp}}$ and $H_{c,\perp} = \frac{2\Phi_0}{\pi D \xi_{\parallel}}$. Consequently, the ratio $H_{c,\parallel}/H_{c,\perp} = \sqrt{2}\xi_{\parallel}/\xi_{\perp}$. However, since ξ depends on the electronic mean free path as $\xi \propto \sqrt{l_e}$, we can again explain the observed anisotropy in the critical field by assuming that l_e is

anisotropic. In terms of the ratio of the critical fields one obtains the same relation $l_e^{\perp}/l_e^{\parallel} \propto (H_{c,\parallel}/H_{c,\perp})^2$. We can therefore conclude that both theoretical approaches give the same predictions.

ACKNOWLEDGMENTS

We acknowledge M. Kröll for the sample fabrication, M.W.J. Crajé and T. van Meerten for sample characterization, F. Luis for help with measurements, D.Y. Vodolazov, F.M. Peeters, S.I. Mukhin, J. Aarts, and P.H. Kes for useful discussions. This work was supported by “Stichting voor Fundamenteel Onderzoek der Materie” (FOM).

*Present address: Energy Research Center of the Netherlands (ECN), Postbus 1, 1755 ZG, Petten, The Netherlands. Email address: otsorop@xs4all.nl

†Corresponding author.

Email address: jongh@physics.leidenuniv.nl

¹A. K. Geim, I. V. Grigorieva, S. V. Dubonos, J. G. S. Lok, J. C. Maan, A. E. Filippov, and F. M. Peeters, *Nature (London)* **390**, 259 (1997).

²J.-M. Duan, *Phys. Rev. Lett.* **74**, 5128 (1995); A. D. Zaikin, D. S. Golubev, A. van Otterlo, and G. T. Zimanyi, *ibid.* **78**, 1552 (1997); Y. Oreg and A. M. Finkel’stein, *ibid.* **83**, 191 (1999); G. Schön, *Nature (London)* **404**, 948 (2000).

³F. Sharifi, A. V. Herzog, and R. C. Dynes, *Phys. Rev. Lett.* **71**, 428 (1993); P. Xiong, A. V. Herzog, and R. C. Dynes, *ibid.* **78**, 927 (1997).

⁴A. Bezryadin, C. N. Lau, and M. Tinkham, *Nature (London)* **404**, 971 (2000); A. Rogachev and A. Bezryadin, *Appl. Phys. Lett.* **83**, 512 (2003).

⁵D. S. Hopkins, D. Pekker, P. Goldbart, and A. Bezryadin, *Science* **308**, 1762 (2005).

⁶S. Michotte, S. Matefi-Tempfli, and L. Piraux, *Appl. Phys. Lett.* **82**, 4119 (2003); D. Y. Vodolazov, F. M. Peeters, L. Piraux, S. Matefi-Tempfli, and S. Michotte, *Phys. Rev. Lett.* **91**, 157001 (2003); G. Stenuit, S. Michotte, J. Govaerts, and L. Piraux, *Eur. Phys. J. B* **33**, 103 (2003); S. Michotte, S. Matefi-Tempfli, L. Piraux, D. Y. Vodolazov, and F. M. Peeters, *Phys. Rev. B* **69**, 094512 (2004).

⁷Ge Yi and W. Schwarzacher, *Appl. Phys. Lett.* **74**, 1746 (1999); S. Yuan, L. Ren, and F. Li, *Phys. Rev. B* **69**, 092509 (2004).

⁸Y. J. Hsu and S. Y. Lu, *J. Phys. Chem. B* **109**, 4398 (2005).

⁹M. L. Tian, J. G. Wang, J. Snyder, J. Kurtz, Y. Liu, P. Schiffer, T. E. Mallouk, and M. H. W. Chan, *Appl. Phys. Lett.* **83**, 1620 (2003); M. L. Tian, J. G. Wang, J. S. Kurtz, Y. Liu, M. H. W. Chan, T. S. Mayer, and T. E. Mallouk, *Phys. Rev. B* **71**, 104521

(2005); H. Wang, M. M. Rosario, N. A. Kurz, B. Y. Rock, M. Tian, P. T. Carrigan, and Y. Liu, *Phys. Rev. Lett.* **95**, 197003 (2005).

¹⁰P. M. Paulus, F. Luis, M. Kröll, G. Schmid, and L. J. de Jongh, *J. Magn. Magn. Mater.* **224**, 180 (2001).

¹¹T. G. Sorop, C. Untiedt, F. Luis, M. Kröll, M. Raşa, and L. J. de Jongh, *Phys. Rev. B* **67**, 014402 (2003); T. G. Sorop, Ph.D. thesis, Leiden University, 2004.

¹²Y. Ishii and M. Sato, *J. Magn. Magn. Mater.* **82**, 309 (1989).

¹³D. J. Griffiths, *Introduction to Electrodynamics*, 2nd ed. (Prentice-Hall, Englewood Cliffs, NJ, 1989).

¹⁴M. Tinkham, *Introduction to Superconductivity*, 2nd ed. (McGraw-Hill, New York, 1995).

¹⁵V. P. Silin, *Zh. Eksp. Teor. Fiz.* **21**, 1330 (1951) (in Russian); for parallel case formulas see, for instance, also O. S. Lutes, *Phys. Rev.* **105**, 1451 (1956) or S. Dubois, A. Michel, J. P. Eymery, J. L. Duvail, and L. Piraux, *J. Mater. Res.* **14**, 665 (1999).

¹⁶Note that in order to keep the relation as simple as possible we have neglected the higher order field terms which are so small that play no role in our case.

¹⁷Silin’s derivations were done for a cylinder of infinite length. In perpendicular field, only the shielding currents running parallel to the long axis of the cylinder were taken into account, neglecting the currents at the end edges. However, as argued by Brandt (Ref. 20), independent of the size of the wire the currents at the edges will give a contribution exactly equal to that from the currents parallel to the long axis. Based on this argument, we have corrected Silin’s formula by multiplying with a factor of 2 the result for M_{\perp} .

¹⁸K. D. Usadel, *Phys. Rev. Lett.* **25**, 507 (1970); A. Anthore, H. Pothier, and D. Esteve, *ibid.* **90**, 127001 (2003).

¹⁹D. Y. Vodolazov (private communication).

²⁰E. H. Brandt, *Phys. Rev. B* **49**, 9024 (1994).